Centromere Locations in *Brassica* A and C Genomes Revealed Through Half-Tetrad Analysis

Annaliese S. Mason,*,†,1 Mathieu Rousseau-Gueutin,‡ Jérôme Morice,‡ Philipp E. Bayer,†,§ Naghmeh Besharat,§ Anouska Cousin,§ Aneeta Pradhan,§ Isobel A. P. Parkin, Anne-Marie Chèvre,‡ Jacqueline Batley,§,† and Matthew N. Nelson§,††,1**

*Department of Plant Breeding, Research Centre for Biosystems, Land Use and Nutrition, Justus Liebig University Giessen, 35392 Giessen, Germany, †School of Agriculture and Food Sciences and Centre for Integrative Legume Research, The University of Queensland, Brisbane 4072, Australia, ‡UMR 1349, Institut de Génétique, Environnement et Protection des plantes, Institut National de la Recherche Agronomique, BP35327, 35653 Le Rheu, France, §School of Plant Biology and The University of Western Australia Institute of Agriculture, The University of Western Australia, Crawley 6009, Western Australia, Australia, **Agriculture and Agri-Food Canada, Saskatoon Research Centre, Saskatoon, S7N 0X2 Saskatchewan, Canada, and ††Natural Capital and Plant Health, Royal Botanic Gardens Kew, Millennium Seed Bank, Wakehurst Place, Ardingly, West Sussex, RH17 6TN, United Kingdom

ABSTRACT Locating centromeres on genome sequences can be challenging. The high density of repetitive elements in these regions makes sequence assembly problematic, especially when using short-read sequencing technologies. It can also be difficult to distinguish between active and recently extinct centromeres through sequence analysis. An effective solution is to identify genetically active centromeres (functional in meiosis) by half-tetrad analysis. This genetic approach involves detecting heterozygosity along chromosomes in segregating populations derived from gametes (half-tetrads). Unreduced gametes produced by first division restitution mechanisms comprise complete sets of nonsister chromatids. Along these chromatids, heterozygosity is maximal at the centromeres, and homologous recombination events result in homozygosity toward the telomeres. We genotyped populations of half-tetrad-derived individuals (from *Brassica* interspecific hybrids) using a high-density array of physically anchored SNP markers (Illumina *Brassica* 60K Infinium array). Mapping the distribution of heterozygosity in these half-tetrad individuals allowed the genetic mapping of all 19 centromeres of the *Brassica* A and C genomes to the reference *Brassica napus* genome. Gene and transposable element density across the *B. napus* genome were also assessed and corresponded well to previously reported genetic map positions. Known centromere-specific sequences were located in the reference genome, but mostly matched unanchored sequences, suggesting that the core centromeric regions may not yet be assembled into the pseudochromosomes of the reference genome. The increasing availability of genetic markers physically anchored to reference genomes greatly simplifies the genetic and physical mapping of centromeres using half-tetrad analysis. We discuss possible applications of this approach, including in species where half-tetrads are currently difficult to isolate.

KEYWORDS recombination; molecular karyotyping; *Brassica*; centromeres; unreduced gametes

IN the age of next-generation sequencing, many new aspects of the genome are being revealed (Metzker 2010). However, certain genomic features still remain recalcitrant to sequence-based analysis. The most obvious of these are repeat sequences; assembly of large repetitive regions using the current generation of technologies is very difficult (Metzker 2010). Unfortunately, these repeat sequences also hide a chromosomal feature of great interest to many geneticists: the centromere. Assembly of centromeric sequences is notoriously problematic (Rudd and Willard 2004), and locating the centromeres on both genetic and physical maps is difficult to achieve (Copenhaver *et al.* 1999). Adding to the complexity, previously active centromeres have been demonstrated to become inactive (no longer functional in meiosis) after chromosome fusion or polyploidization events (Han *et al.* 2006),

doi: 10.1534/genetics.115.183210
Manuscript received September 28, 2015; accepted for publication November 23, 2015; published Early Online November 25, 2015.
Supporting information is available online at www.genetics.org/lookup/suppl/doi:10.1534/genetics.115.183210/-/DC1.
[1]Corresponding authors: Department of Plant Breeding, IFZ Research Centre for Biosystems, Land Use and Nutrition, Justus Liebig University, Heinrich-Buff-Ring 26-32, 35392 Giessen, Germany. E-mail: annaliese.mason@agrar.uni-giessen.de; and Natural Capital and Plant Health, Royal Botanic Gardens, Kew, Wakehurst Place, Ardingly, West Sussex, RH17 6TN, United Kingdom. E-mail: m.nelson@kew.org

and active centromeres do not always have associated sequence-based motifs (Nasuda *et al.* 2005; Zhang *et al.* 2010).

Genetic mapping of centromeres using tetrads or half-tetrads avoids these sequence-based pitfalls. Tetrad analysis was developed in fungi (Mather and Beale 1942), but has been rarely applied to locate functional centromeres in plant genomes, with *Arabidopsis thaliana* being the most notable exception (Copenhaver *et al.* 1999). The physical location of functional centromeres on reference genomes can be inferred from genetic map positions via physically anchored markers (Copenhaver *et al.* 2000). Full-tetrad analysis in plants is contingent on the availability of mutants where tetrads fail to disassociate during pollen development (Copenhaver *et al.* 2000). Pollen tetrads have been reported in hundreds of species to date (Copenhaver 2005); however, manual isolation of individual tetrads can be challenging (Copenhaver *et al.* 2000; Ludlow *et al.* 2013). Half-tetrad analysis may be more readily applicable: unreduced (2n) gametes have been reported in a wide range of plant and animal species (Ramsey and Schemske 1998). The frequency of unreduced gametes is low in most species, but can be enriched in populations derived from interspecific, interploid or translocation hybrids (Ramsey and Schemske 1998; Ramanna and Jacobsen 2003; Mason *et al.* 2011b). Unreduced gamete production can also often be induced or enhanced by environmental stimuli (Ramsey and Schemske 1998; Mason *et al.* 2011b; De Storme *et al.* 2012). Half-tetrad analysis has been carried out in a number of animal species to map centromeres: zebrafish (Johnson *et al.* 1995), cape honeybee (Baudry *et al.* 2004), abalone (Nie *et al.* 2012), Japanese eel (Nomura *et al.* 2006), oyster (Hubert *et al.* 2009), carp (Liu *et al.* 2013), turbot flatfish (Martinez *et al.* 2008), and sea cucumber (Nie *et al.* 2011). Plant species centromeres have been genetically mapped using half-tetrad analysis in maize (Schneerman *et al.* 1998; Lin *et al.* 2001), alfalfa (Tavoletti *et al.* 1996), mandarin (Cuenca *et al.* 2011; Aleza *et al.* 2015), and potato (Park *et al.* 2007).

Many different mechanisms of unreduced gamete formation exist [reviewed by Bretagnolle and Thompson (1995), Brownfield and Köhler (2011), and Veilleux (1985)]. For half-tetrad analysis, unreduced gametes must be produced by either a first-division restitution-like mechanism (FDR) or a second-division restitution-like mechanism (SDR) that in both cases permits homologous chromosome pairing at metaphase I. In FDR, the first meiotic division fails to separate nonsister chromatids, resulting in a mitosis-like division (but often with homologous chromosome pairing). In SDR, the second meiotic division fails to separate sister chromatids. The principle of centromere mapping relies on the fact that in FDR, both centromeres of each pair of nonsister chromatids are transmitted to the resulting gamete, resulting in perfectly heterozygous centromere regions in every gamete. Recombination events convert distal chromosome locations from heterozygous to homozygous states. Therefore, across the FDR gamete population the frequency of heterozygosity decreases as the distance from the centromere increases, due to homologous recombination events. In half-tetrad analysis via SDR (failure of meiosis to separate sister chromatids), both centromeres of each pair of sister chromatids are transmitted to the resulting gamete. This results in perfectly homozygous centromere regions in every SDR gamete, but with increasing heterozygosity toward the telomeres across the SDR gamete population due to homologous recombination events.

In previous half-tetrad analyses, centromere locations were mapped using low-throughput marker (*e.g.*, microsatellite) genotyping of populations derived from interploid crosses or chromosome translocation hybrids (Zhao and Speed 1998). In the absence of reference genome sequences, these studies used either highly sophisticated mapping algorithms or a two-step approach whereby markers were first allocated to positions on chromosomes and then heterozygosity levels were independently mapped to identify centromere locations (Zhao and Speed 1998). This technical complexity, along with the relatively few systems with reproducibly high frequencies of unreduced gametes, may in part explain why comparatively few species have currently undergone half-tetrad analysis.

Here we demonstrate how current genomic technologies can be applied for very simple mapping of centromeres, using markers of known genomic locations. Using the recently released Illumina Infinium 60K SNP chip for *Brassica napus*, we undertook centromere mapping in a population cultured from unreduced microspores of *B. napus* × *B. carinata* hybrids (genome configuration CCAB), and *B. juncea* × *B. napus* hybrids (genome configuration AABC). Our results for half-tetrad mapping of the C-genome chromosomes using a smaller population were reported previously in Parkin *et al.* (2014). Here, we describe our method in full and report its application to the A-genome and to larger C-genome populations (providing greater resolution) and the results of a sequence-based centromere placement approach. All active *Brassica* centromeres were physically mapped to the 10 A- and 9 C-genome chromosomes in the recently released *B. napus* reference genome sequence (Chalhoub *et al.* 2014) using half-tetrad analysis.

Materials and Methods

Experimental material

The experimental material comprised populations derived by two different methods: microspore culture (to map both A- and C- genome centromeres) and test crosses (C-genome centromeres only). An overview of the methods used to generate the experimental material is provided in Figure 1.

To generate the novel A-genome mapping population, four different *B. juncea* × *B. napus* first generation interspecific hybrids (AABC genome configuration; Supporting Information, Table S1) were cultured to produce 86 total microspore-derived progeny. These progeny sets contained 20, 23, 23, and 20 individuals, respectively. Microspore culture was carried out according to protocols detailed in Takahira *et al.* (2011).

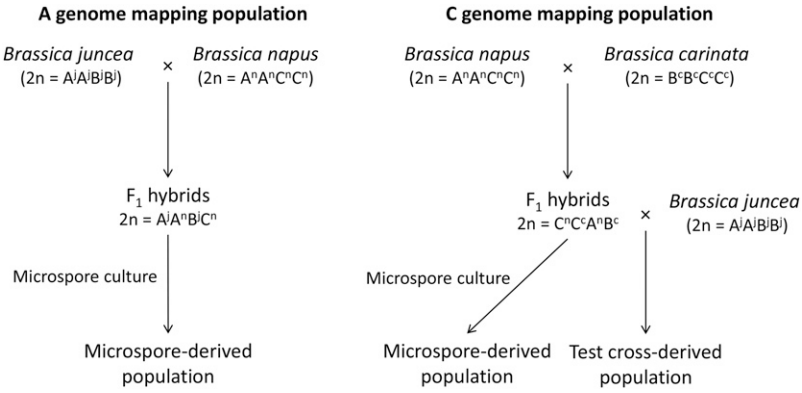

Figure 1 Overview of the methods used to obtain unreduced gamete-derived individuals to map the *Brassica* A- and C-genome centromere locations.

For C-genome mapping, microspore-derived progeny from CCAB hybrids were from two different groups. The first group comprised a population of 81 individuals derived from gametes of *B. napus* × *B. carinata* hybrids (CCAB genome) via microspore culture. Detailed information about the production of this population was provided by Nelson *et al.* (2009) and Mason *et al.* (2011a). In Mason *et al.* (2011a) SNP genotyping was carried out for DNA samples from the 57 plants in 10 progeny sets identified as (1) resulting from unreduced gametes and (2) having nonidentical haplotypes. The results from this set of individuals were previously reported in Parkin *et al.* (2014). The second group (new to this study) comprised a population of 75 individuals also derived from gametes of *B. napus* × *B. carinata* hybrids (CCAB genome) via microspore culture. This population was generated at The University of Western Australia following protocols detailed in Takahira *et al.* (2011) as above. Four different interspecific hybrid genotypes were cultured to produce 18, 16, 23, and 18 progeny, respectively (Table S1).

Also for C-genome mapping, a novel third population of 65 individuals was produced through test crossing of six *B. napus* × *B. carinata* interspecific hybrid genotypes (CCAB genome composition) to *B. juncea* (six progeny sets, Table S1). Crossing was carried out according to methods detailed in Mason *et al.* (2012), using the *B. napus* × *B. carinata* hybrid as the female parent in the cross.

Marker genotyping and half-tetrad analysis to identify centromere locations

Genomic DNA was extracted from embryos, cotyledons, or true leaves of the progeny sets following the method of Chen *et al.* (2008) for the microspore-derived embryos and following the microprep method of Fulton *et al.* (1995) for the cross-progeny. The *Brassica* 60K Infinium array (Illumina, San Diego) was used to generate SNP marker data for the experimental populations, parental species, and *B. napus* × *B. carinata* and *B. juncea* × *B. napus* interspecific hybrid controls (Mason *et al.* 2014a). Data were visualized in Genome Studio (Illumina). In total, 7,168 A-genome-specific SNP markers and 13,819 C-genome-specific SNP markers were polymorphic between the two parent genotypes of at least one progeny set in the experimental population and could be uniquely located on the *B. napus* "Darmor" reference sequence (Chalhoub *et al.* 2014). This resulted in an average SNP density of one SNP every 42 kbp in the A genome and one SNP every 36 kbp in the C genome. Putatively multilocus SNP markers (as evidenced by heterozygosity in the homozygous parent lines or by multiple genotype clusters in Genome Studio) and SNPs with haplotype patterns not matching the chromosome on which they were putatively located were removed from the analysis [see Mason *et al.* (2014a) for a detailed description of this method]. SNP markers that were monomorphic between parent genotypes within a progeny set were set as missing values. Missing values in haplotype blocks were imputed from flanking markers when available and to the ends of chromosomes. Resulting percentage of heterozygosity in each haplotype block across the population was plotted for each chromosome to identify "peaks" of high heterozygosity in FDR unreduced gamete-derived individuals putatively representing the genetic centromere locations. SNPs with the maximum heterozygosity for each chromosome were assumed to be within the centromere region. The first SNP marker to show decreased heterozygosity in the direction of each telomere was taken as a flanking marker for the centromere boundary. SNP marker locations were derived from the published *B. napus* Darmor genome sequence (Chalhoub *et al.* 2014) using the best match from BLAST alignments of the 50-bp probe sequences (95% sequence identity, no gaps permitted).

Location of B. napus centromere- and pericentromere-specific repeats

The (peri)centromere-specific repeat sequences CentBr1 and CentBr2 (176-bp centromere satellite repeats) were retrieved from the BAC end sequences of the *B. rapa* clones KBrH001B09 (GenBank accession CW978699) and KBrH001E07 (GenBank accession CW978837), respectively (Lim *et al.* 2005; Koo *et al.* 2011). These two sequences were blasted (*e*-value: 10^{-6}) against the *B. napus* (Darmor v4.1) genome sequence (Chalhoub *et al.* 2014) using BLASTn (Altschul *et al.* 1990). Only BLAST results with at least 90% sequence similarity to the *B. napus* genome were kept for each CentBr sequence, as the different copies of each class have >90% sequence similarity, while CentBr1 and CentBr2 present ~82% sequence similarity (Lim *et al.* 2005). In addition, BLASTn was used to align sequences (against the *B. napus*

genome) that are found in the pericentromeric heterochromatin blocks of *Brassica* chromosomes (Lim *et al.* 2007). These comprised a centromere-specific Ty1/copia-like retrotransposon of *Brassica* (CRB, BAC KBrH00P13: GenBank accession AC166739); a 238-bp degenerate tandem repeat (TR238, BAC KBrH015B20: GenBank accession AC166740); and an 805-bp tandem repeat (TR805, BAC KBrH00P13: GenBank accession AC166739). Subsequently, only BLAST results presenting at least 90% identity and a minimal alignment length of 20% were considered [a low stringency was used to improve the chance of detecting these difficult-to-assemble repeat sequences, in line with the methodology of Cheng *et al.* (2013)]. Finally, attempts were made to physically localize centromere-specific histone H3 variant using the partial *B. napus* CenH3 cDNA clone sequences [GenBank accession HM582931, HM582932, HM582933, HM582934, HM582935, HM582936, HM582937, and HM582938; Wang *et al.* (2011)], by performing a BLASTp alignment against Darmor amino-acid gene-coding sequences (Chalhoub *et al.* 2014). The physical locations of these various (peri)centromere-specific sequences on the *B. napus* (Darmor) genome were represented graphically (Figure 2, outer circle) using Circos software (Krzywinski *et al.* 2009).

Gene and transposable element density

To determine the gene density on each *B. napus* chromosome, the start and end position of each of the 101,0140 gene sequences (messenger RNA, mRNA) identified in *B. napus* Darmor by Chalhoub *et al.* (2014) and available from the Genoscope website (http://www.genoscope.cns.fr/brassicanapus/data/) were recovered. For each chromosome, the gene density was defined using a sliding 1-Mb window; for each window, the gene density was calculated by dividing the number of nucleotides annotated as gene sequences by the size of the window (1,000,000 bp). Similarly, the density of transposable elements (TEs) was calculated using the total number of nucleotides annotated as TE divided by the size of the window (1,000,000 bp) (Chalhoub *et al.* 2014).

Data availability

Genotypes and production methods to obtain 2n-gamete derived progeny are presented in Table S1. Detailed information related to the centromere positions and flanking SNP marker locations on the genome reference sequence is presented in Table S2. Sequence information produced by Chalhoub *et al.* 2014 used to generate the Circos plot is available from the Genoscope website (http://www.genoscope.cns.fr/brassicanapus/data/).

Results

Production of unreduced gamete-derived individuals through test crossing and microspore culture

A total of 86 individuals were generated from microspore culture of four different *B. juncea* × *B. napus* interspecific hybrids (same *B. juncea* parent, four different *B. napus*; AABC genome; Table S1). Two pairs of twins were observed from marker results. These plants may have resulted from secondary embryogenesis generating identically twinned embryos during the tissue culture process (Raemakers *et al.* 1995; Cousin and Nelson 2009); one of each pair was removed from the analysis. Of the remaining 84 individuals, 75 (89%) were heterozygous at 38–86% (average 68%) of loci in the A genome; heterozygosity was assessed as presence of both a *B. juncea* and a *B. napus* parental allele at a single A-genome locus (Figure 2A). These were considered to be derived from unreduced AABC gametes from the hybrid parent via first-division restitution-like mechanisms, where nonsister chromatids assorted into the same gamete after meiosis. The remaining nine individuals were heterozygous at 6–15% of loci in the A genome (Figure 2A). These were considered to be derived from reduced gametes (residual heterozygosity may have resulted from nonhomologous recombination events), or from second division restitution, and were spread evenly among the four progeny sets (Table S1). After removal of clones and reduced gamete-derived individuals, 75 unique experimental individuals were obtained for the A-genome mapping population (87% of microspore-derived progeny).

Both microspore culture and test crosses were used to generate unreduced gamete-derived progeny from *B. napus* × *B. carinata* interspecific hybrids (CCAB genome). A total of 124 microspore-derived progeny and 65 test-cross progeny were produced from 14 different genotype combinations (Table S1).

Of the 57 microspore-derived plants in 10 progeny sets with nonidentical haplotypes in Mason *et al.* (2011a), an additional eight individuals were conservatively excluded for this study after SNP marker genotyping revealed that they may have been clones (>95% similar genetic identity) (Raemakers *et al.* 1995; Cousin and Nelson 2009) (Table S1). An additional four clone pairs were also identified in the new microspore-derived progeny, and one of each pair was excluded from further analysis. Of the remaining microspore-derived progeny, 74% (80/112) were heterozygous at 29–97% of C-genome loci, where heterozygosity was assessed as presence of both a *B. napus* and a *B. carinata* allele (average 76%) (Figure 2B). These individuals were therefore concluded to be derived from unreduced CCAB gametes via a first division restitution mechanism. The remaining microspore-derived progeny had 4.5–19% of loci heterozygous for *B. napus* and *B. carinata* alleles (average 7.6%) and were assumed to be derived from reduced gametes (or from second division restitution) [Figure 2B; the 13 reduced gamete-derived individuals from Mason *et al.* (2011a) were not regenotyped using the SNP array and are hence not included in the figure, but showed 0–16% heterozygosity based on SSR markers]. In total, 65% of microspore-derived progeny were unique and derived from unreduced gametes via a first-division restitution-like mechanism.

Of the test-cross progeny from *B. napus* × *B. carinata* interspecific hybrids (CCAB genome) crossed with *B. juncea*, 51% (34/67) were 45–100% heterozygous for parent

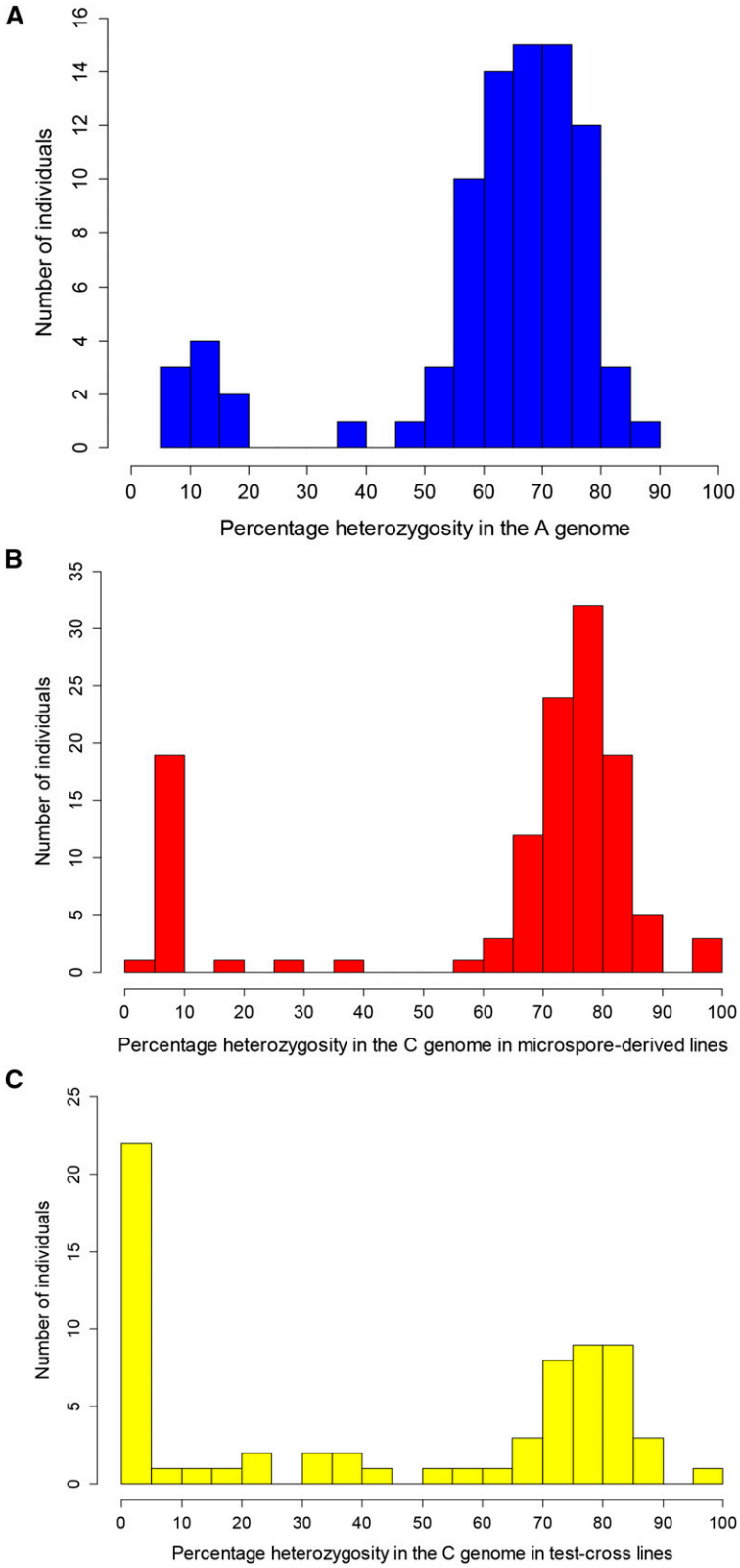

Figure 2 Percentage of heterozygosity as assessed by presence of both parental alleles at a single locus in the diploid genome in individuals derived from (A) microspore culture of *B. juncea* × *B. napus* (2n = AABC) interspecific hybrids; (B) microspore culture of *B. napus* × *B. carinata* (2n = CCAB) interspecific hybrids; and (C) test crosses between *B. napus* × *B. carinata* (2n = CCAB) interspecific hybrids and *B. juncea*.

B. napus and *B. carinata* alleles in the C genome (average 77%) (Figure 2C). These were therefore determined to be derived from CCAB unreduced gametes from the hybrid parent via a first-division restitution-like mechanism. Of the remaining test-cross progeny, 25/67 had 0–25% heterozygosity (average 4%) and were assumed to be derived from reduced gametes from the CCAB parent (Figure 2C). The residual heterozygosity was assumed to result from nonhomologous

Table 1 Locations of the *Brassica* A- and C-genome centromeres

Chromosome	Start (Mbp)	End (Mbp)	Size of centromere-containing region (Mbp)*	Chromosome length (Mbp)**
A01	13.1	14.1	1.0	23.1
A02	13.9	14.2	0.3	24.7
A03	28.0	29.7	1.7	29.7
A04	5.8	6.3	0.5	19.1
A05	10.9	10.9	0.07	23.0
A06	11.1	11.1	0.02	24.3
A07	3.3	5.2	1.9	24.0
A08	3.9	5.2	1.4	18.9
A09	15.6	15.9	0.3	33.7
A10	2.9	5.3	2.4	17.3
C1	17.9	24.2	6.2	38.3
C2	31.8	32.2	0.3	46.1
C3	40.6	41.9	1.3	60.6
C4	17.1	19.4	2.3	48.9
C5	17.6	28.3	10.7	42.6
C6	8.0	8.4	0.5	37.2
C7	5.4	7.2	1.8	44.5
C8	5.8	6.4	0.6	38.3
C9	23.1	23.4	0.3	48.4

* Represents the conservative outer boundaries within which the active centromeric region must fall. SNPs with the maximum heterozygosity for each chromosome were assumed to be within the centromere region. The first SNP marker to show decreased heterozygosity in the direction of each telomere was taken as a flanking marker for the centromere boundary.

** As covered by polymorphic SNP markers in the assembled *B. napus* Darmor v4.1 reference genome sequence (Chalhoub *et al.* 2014).

recombination events. Another 8 individuals had 34–58% heterozygosity (Figure 2C) but contained multiple whole chromosomes that were completely heterozygous or completely homozygous and were unable to be classified as derived from standard FDR, SDR, or reduced gametes (two may have resulted from SDR with minor additional abnormalities), and hence were not included in the half-tetrad analysis.

Locations of the active centromeres deduced by half-tetrad analysis

SNP markers with known physical locations in the *B. napus* genome and peaks of heterozygosity within each chromosome were used to determine the genetic locations of functional centromeres (Table 1, Figure 3, Table S2). Centromeric regions were delineated based on the SNP marker haplotypes containing the highest proportion of heterozygosity on each chromosome, and a conservative estimate of the chromosome region containing the centromere was obtained for each of the 19 *Brassica* chromosomes. The size of the centromere-containing region delineated on the reference genome sequence ranged from 20 kbp to 10.7 Mbp (average 1.8 Mbp; Table 1). These regions were strongly correlated with observable peaks and troughs in TE and gene density, respectively (Figure 3).

Distribution of polymorphic SNP markers and haplotype-based inferences

SNP markers that were polymorphic and amplified only a single locus in the genotypes used in our study were distributed across the *B. napus* Darmor reference genome. A lower density of useable polymorphic SNP markers was found around the centromere regions for all A-genome chromosomes except A04 and A10 and for all C-genome chromosomes except C2, C4, and C6. Most chromosomes appeared to have small physical regions of reduced polymorphism around centromeres based on SNP marker distribution on the Illumina Infinium *Brassica* 60K array, with the exception of chromosomes A02 and C5.

Surprisingly, one progeny set did not show inheritance of chromosome A10 expected from homologous recombination between *B. napus* and *B. juncea*. Instead, the unrecombined *B. napus* parent chromosome was present in 8/22 individuals with no *B. juncea* alleles present, and hence no centromere region could be identified in these individuals. As well, four large (>3 Mbp) putative inversions were observed based on haplotype analysis of all genotypes used in this study relative to the *B. napus* Darmor reference genome sequence. These ranged from 4.62 to 6.01 Mbp in size and were located over the centromere regions on chromosomes C1, C2, and C7 (Table S2). One additional putative inversion was present in only two progeny sets and comprised a 7.90-Mbp region on chromosome C5 (Table S2). Several other smaller putative inversions or rearrangements (<3 Mbp) were also identified and are listed in Table S2.

Distribution of known Brassica centromeric and pericentromeric sequences in the B. napus genome

A total of 206 sequences for CentBr1 and 710 sequences for CentBr2 were identified in the *B. napus* genome using the criteria of >90% identity and >20% alignment length. Of these, only 26% (56) and 58% (415) of CentBr1 and CentBr2 sequence locations, respectively, were on assembled

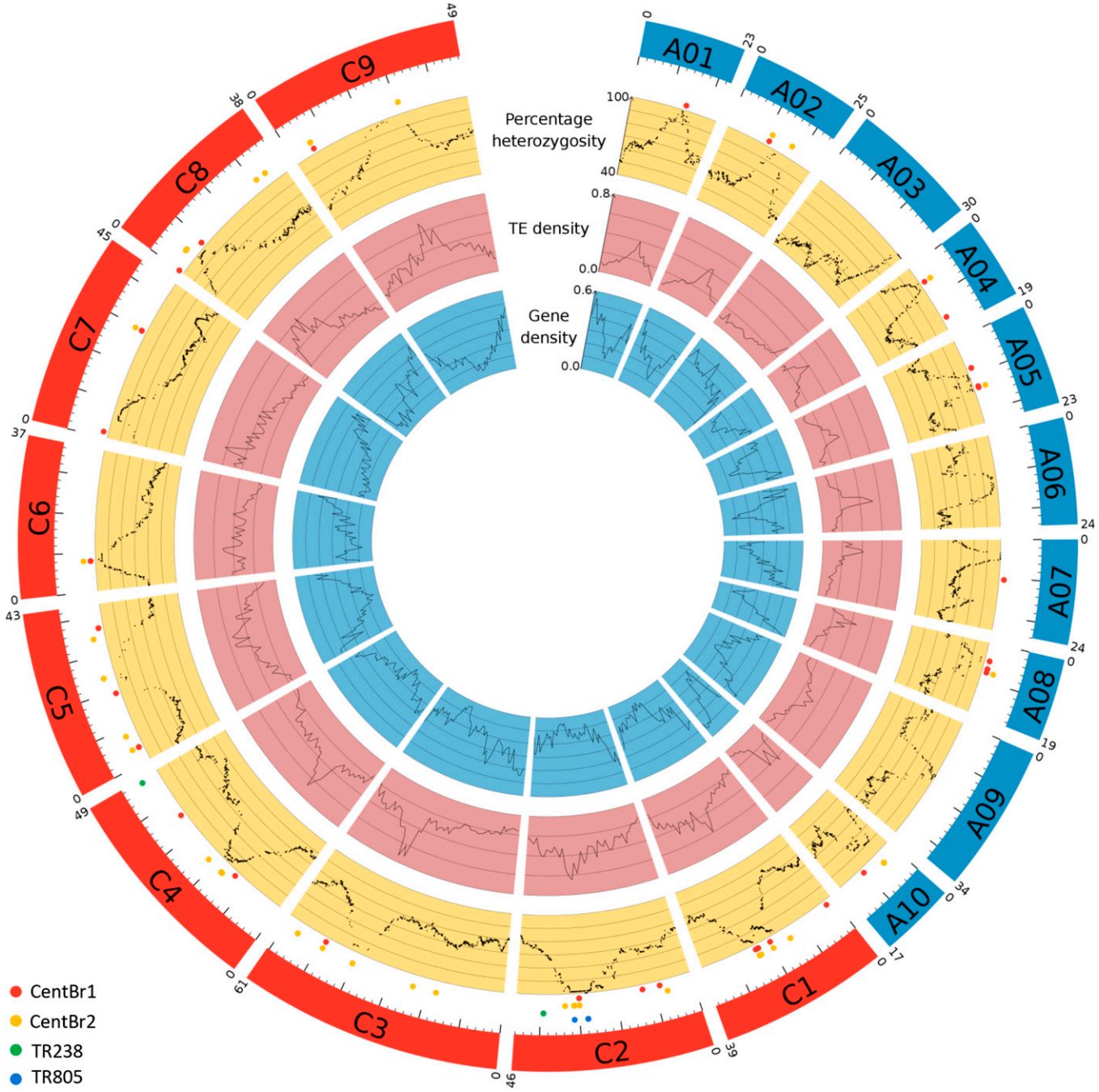

Figure 3 Gene density, TE density, and percentage of heterozygosity (the latter in a population derived from first-division restitution-type unreduced gametes) along each *B. napus* chromosome represented in a Circos plot (Krzywinski *et al.* 2009). The *B. napus* chromosomes belonging to the A and C subgenomes are in blue and red, respectively. The size of each chromosome in megabase pairs is indicated above each chromosome and a ruler is drawn underneath each chromosome, with larger tick marks every 10 Mbp and smaller tick marks every 2 Mbp. Locations of active centromeres are visible as peaks of increased heterozygosity, increased TE density, and decreased gene density. Dots indicate BLAST-located centromeric and pericentromere sequences: CentBr1 sequences (red), CentBr2 sequences (yellow), TR238 sequences (green), and TR805 sequences (blue).

chromosomes. Most of these CentBr2 signals were predominantly localized on chromosomes A10 (88% of the BLAST results specifically located on A pseudochromosomes as opposed to unanchored scaffolds) and C4 (71% of the BLAST results specifically located on C pseudochromosomes). A total of 14 of the 19 A- and C-genome chromosomes had either a CentBr1 or CentBr2 sequence identified in the putative genetic centromere region (Figure 3). However, only chromosomes C6 and A01 contained CentBr sequences solely in the active centromere region, rather than also being present in other locations along the chromosome (Figure 3).

A total of 197 TR238 sequences, 18 TR805 sequences, and 4 CRB sequences were identified, of which 2 (1%), 4 (22%), and none could be mapped to assembled chromosomes. The four TR805 sequences localized to the C2 genetic centromere region, whereas the two sequences from TR238 were not found in active centromere regions (Figure 2). The eight CENH3 query protein sequences all aligned to a single location in the *B. napus* genome that was on an unanchored C chromosome location. This *B. napus* protein sequence was identical to one of the CENH3 query proteins (GenBank accession HM582935).

Discussion

Based on genomic sequence information from *B. napus*, we located the 19 active *Brassica* A- and C-genome centromeres on the reference genome. This was achieved by high-resolution genotyping of populations of microspore- and test-cross-derived progeny generated from unreduced gametes of interspecific *Brassica* hybrids. With the increasing availability of high-throughput genotyping methodologies and reference genome sequences, this half-tetrad mapping approach can be readily carried out to locate centromeres in other species of interest known to produce unreduced gametes.

The physical size of the centromere regions in *A. thaliana* ranges from 0.5 to 1.79 Mbp (Copenhaver *et al.* 1999; Hosouchi *et al.* 2002). Assuming that centromere size is similar or greater in *B. napus*, and from the fact that the majority of centromere-specific sequences did not find matches in the assembled pseudochromosomes, we expect that the majority of the centromere regions in the *B. napus* reference genome sequence are not yet assembled and/or genetically anchored. This is not unexpected, due to the difficulty in assembling the complex repetitive elements that make up these regions using next-generation sequencing approaches. However, for all centromeric regions there were distinctive patterns in the surrounding genome sequence that provide additional landmarks indicating their presence, in particular, an observable drop in gene density and generally a concomitant increase in TE density (Figure 3). Centromeres C4 and A10 appear to be the most represented centromere regions in the current reference genome sequence, based on the number of localized repeats (the majority of CentBr sequences identified were on these two chromosomes). The observation of CentBr sequence alignments outside the predicted genetic centromeres may represent small-scale misplacements of these particular scaffolds relative to the reference genome sequence. Alternatively, these could represent defunct centromere regions remaining after the *Brassica* polyploidization events (Cheng *et al.* 2013), or the repeat sequences may simply not underlie the active centromeres, as centromeric repeats are not always necessary for centromere activity (Nasuda *et al.* 2005; Liu *et al.* 2015).

The physically anchored genetic centromere locations identified here correlated with the chromosome structures reported previously using cytogenetic methods (Olin-Fatih and Heneen 1992; Cheng *et al.* 1995; Xiong and Pires 2011). Chromosomes C7 and C8 had subterminal centromeres, and the remainder of the C-genome chromosomes approximately median or submedian centromeres, supporting the molecular cytogenetic karyotyping of Xiong and Pires (2011). The orientation of chromosomes in the C-genome reference sequence is based on the reference genetic map of Parkin *et al.* (1995) and Parkin *et al.* (2014). Here we confirm the previous proposal by Howell *et al.* (2002) that several C-genome linkage groups (*e.g.*, C2 and C3) were inverted, relative to the convention of orienting chromosomes with the short arm on top and long arm at the bottom. Further validation of these results is pending a more complete genome assembly. Koo *et al.* (2004) identified two median, five submedian, two subtelocentric, and one acrocentric centromere in the *B. rapa* genome; Xiong and Pires (2011) show chromosome A07 as acrocentric and A04 and A10 as subtelocentric, reasonably congruent with our results (Table S2). Chromosomes A01, A02, and A03 in the current genome reference sequence were inverted relative to the "short arm on top" convention, most significantly for A03 with centromere positioned at the end of the chromosome assembly. Hence, our centromere-positioning analysis suggests that the short arm of chromosome A03 has not been assembled in the published Darmor reference genome. This is not surprising as the short arm of chromosome A03 is a known nucleolar organizing region (NOR), composed of repetitive elements and arrays; Mun *et al.* (2010) were also unable to identify any BACs localized to this chromosome arm in their sequence and assembly of A03.

Cheng *et al.* (2013) performed an extensive investigation of paleocentromeres in *B. rapa* using a sequence-based approach. Their placement of 8/10 A-genome centromeres corresponded perfectly to our identified genetic centromeres; only for chromosomes A02 and A09 was an inactive region selected as the active centromere (and for both A02 and A09 a "trace" centromere region was identified by Cheng *et al.* (2013), which aligned with our active genetic centromere region). This result supports the utility of half-tetrad analysis in identifying active *vs.* paleocentromeres, but also shows that combining both sequence-based and genetic mapping-based approaches can yield the most useful genomic information. This was also demonstrated by the close correlations between the placement of the centromeres using TE and gene density and the placement using the half-tetrad mapping approach in our study.

Several large inversions and a number of small rearrangements were observed in our study based on haplotype analysis relative to the *B. napus* Darmor reference genome. Chromosomes C1, C2, and C7 all had large inversions over the centromere region (Table S2); for chromosome C1 (and to a lesser extent C2) this was directly observable as the presence of two peaks of heterozygosity (instead of one peak) indicating the centromere region (Figure 3). These rearrangements may result from actual genotypic differences between the genotypes used in this experiment and Darmor

or from misassembly of the *B. napus* genome sequence. The lack of resolution of the C5 centromere in our study may also be related to putative chromosome structural rearrangements between the parents of our mapping populations, as few polymorphic SNPs were identified between our parent lines for this region; but SNPs were present in this region on the array. Future validation using a wider range of genotypes could be helpful to confirm this and to improve the accuracy of the C5 centromere mapping. The accurate genetic anchoring and orienting of sequenced scaffolds closely associated with centromeres is often impeded by limited recombination in the proximity of the centromere. Differences between genotypes for SNP probe specificity may also cause differences between our results and the reference genome sequence. However, such differences are more likely to result in A- or C-genome probe aspecificity (*e.g.*, amplification of a homeologous region in our lines, instead of the region in the reference identified through BLAST) than inversions and small-scale rearrangements. Further investigation of the genotypic variation for chromosome rearrangements present within *B. napus* would be useful in confirming our observations. Although a number of homeologous translocation events have been previously characterized in *B. napus* (Osborn *et al.* 2003), the recent availability of a reference genome sequence and high-throughput genotyping tools such as the Illumina Infinium *Brassica* 60K array is expected to shed light on the *B. napus* core and disposable genome.

We used both microspore culture and test crosses to produce unreduced gamete-derived individuals for half-tetrad analysis (Nelson *et al.* 2009; Mason *et al.* 2011a). Although microspore culture is not practicable in most species, unreduced gametes are also commonly observed in interspecific and interploid hybrids (Ramsey and Schemske 1998; De Storme and Mason 2014; Mason and Pires 2015), which can be used to generate suitable populations in a wider range of species through test-cross approaches. In our study, both test-crossing and microspore culture yielded >50% unreduced gamete-derived progeny using a number of different interspecific hybrid genotypes. It is interesting to note that test crossing of a single genotype of *B. juncea* × *B. napus* interspecific hybrid to two genotypes of *B. carinata* in a previous study yielded only reduced gamete-derived individuals (Mason *et al.* 2012). In this study, the same hybrid genotype of *B. juncea* × *B. napus* was successfully used to generate 87% unreduced gamete-derived progeny through microspore culture (Table S1, A_MD_03). This supports previous research that microspore culture preferentially selects unreduced gametes in interspecific *Brassica* hybrids (Nelson *et al.* 2009; Mason *et al.* 2011a).

Progeny were most commonly derived from first division restitution-like mechanisms: an example mechanism is parallel spindles at meiosis II, which has previously been observed in these *Brassica* hybrids (Nelson *et al.* (2009); however, many such mechanisms exist [see Bretagnolle and Thompson (1995); De Storme and Geelen (2013), and De Storme and Mason (2014)]. The common observation of FDR rather than SDR is not surprising: in these AABC and CCAB hybrid types, FDR produces gametes with a similar chromosome composition to the parents, but SDR results in either zero or two copies of single copy (univalent) chromosomes, with probable detrimental effects on viability. The observation of what appears to be indeterminate meiotic restitution [where some homologous chromosomes separate and some sister chromatids separate, but not all; see Lim *et al.* (2001) for a description of this phenomenon] in some of the test-cross progeny was surprising, but this form of meiotic restitution has also been observed previously in other species and hybrid types (Lim *et al.* 2001; Ramanna and Jacobsen 2003). Another explanation for the failure to detect heterozygous regions for some centromeres may be the undetected occurrence of double cross-over events (a cross-over on either side of the centromere) very close to the centromere region, where SNP marker coverage was poor and the genome assembly more likely to contain gaps.

The *Brassica* model is unusually amenable for generating interspecific hybrids in many combinations of A, B, and C genomes (Chen *et al.* 2011), with largely regular chromosome pairing and segregation between homologous chromosomes derived from different species (Leflon *et al.* 2006; Mason *et al.* 2014b). However, even in this system we found an unusual example of failure of homologous *Brassica* chromosomes to segregate normally. The microspore-derived progeny of hybrid genotype A_MD_02 (Table S1) failed to show expected segregation patterns and recombination between chromosome A10 from *B. napus* and chromosome A10 from *B. juncea*. Missegregation of homologous chromosomes is thought to be uncommon but has been observed occasionally in *Brassica* interspecific hybrid types (Mason *et al.* 2015), and such meiotic abnormalities may occur more frequently in interspecific hybrids of other plant genera (De Storme and Mason 2014). The failure to detect heterozygosity associated with the A10 centromere in several individuals from one genotype group in this study may also be related to the presence of a genotype-specific chromosome rearrangement; this could either hinder pairing between the homologous chromosomes or hinder detection of cross-over events over the centromere region.

Interspecific hybrids are an extremely common phenomenon in many genera (Mallet 2007). The tendency for interspecific hybrids to produce high frequencies of unreduced gametes is not only frequently observed (Ramsey and Schemske 1998), but is predicted to be moderately universal, due to the common chromosome mechanics involved [for a review see De Storme and Mason (2014) and De Storme and Geelen (2013)]. This study demonstrates the utility of both test crosses and microspore culture in generating unreduced gamete-derived progeny from interspecific hybrids: such approaches should also be feasible in other genera. In future, as single-molecule genome sequencing technologies become available, it may also become possible to sequence unreduced gametes sorted by size using flow cytometry (Pan *et al.* 2004;

De Storme *et al.* 2013), bypassing the often technically challenging stage of developing an adult population and offering a potential avenue for half-tetrad analysis in an even broader range of species.

Acknowledgments

We thank Shyam Sundar Dey for assistance with microspore culture. Rowan Bunch is gratefully acknowledged for Illumina HiScan SNP chip scanning. This work was supported by an Australian Research Council Discovery Early Career Researcher Award (DE120100668); Emmy Noether Deutsche Forschungsgemeinschaft grant MA 6473/1-1; and Australian Research Council Project grants LP0883642, DP0985953, and LP110100200.

Literature Cited

Aleza, P., J. Cuenca, M. Hernandez, J. Juarez, L. Navarro *et al.*, 2015 Genetic mapping of centromeres in the nine *Citrus clementina* chromosomes using half-tetrad analysis and recombination patterns in unreduced and haploid gametes. BMC Plant Biol. 15: 80.

Altschul, S. F., W. Gish, W. Miller, E. W. Myers, and D. J. Lipman, 1990 Basic Local Alignment Search Tool. J. Mol. Biol. 215: 403–410.

Baudry, E., P. Kryger, M. Allsopp, N. Koeniger, D. Vautrin *et al.*, 2004 Whole-genome scan in thelytokous-laying workers of the cape honeybee (*Apis mellifera capensis*): central fusion, reduced recombination rates and centromere mapping using half-tetrad analysis. Genetics 167: 243–252.

Bretagnolle, F., and J. D. Thompson, 1995 Tansley review No. 78. Gametes with the stomatic (*sic*) chromosome number: mechanisms of their formation and role in the evolution of autopolyploid plants. New Phytol. 129: 1–22.

Brownfield, L., and C. Köhler, 2011 Unreduced gamete formation in plants: mechanisms and prospects. J. Exp. Bot. 62: 1659–1668.

Chalhoub, B., F. Denoeud, S. Y. Liu, I. A. P. Parkin, H. B. Tang *et al.*, 2014 Early allopolyploid evolution in the post-Neolithic *Brassica napus* oilseed genome. Science 345: 950–953.

Chen, S., M. N. Nelson, K. Ghamkhar, T.-d. Fu, and W. A. Cowling, 2008 Divergent patterns of allelic diversity from similar origins: the case of oilseed rape (*Brassica napus* L.) in China and Australia. Genome 51: 1–10.

Chen, S., M. N. Nelson, A.-M. Chèvre, E. Jenczewski, Z. Li *et al.*, 2011 Trigenomic bridges for *Brassica* improvement. Crit. Rev. Plant Sci. 30: 524–547.

Cheng, B. F., W. K. Heneen, and B. Y. Chen, 1995 Mitotic karyotypes of *Brassica campestris* and *Brassica alboglabra* and identification of the *B. alboglabra* chromosome in an addition line. Genome 38: 313–319.

Cheng, F., T. Mandakova, J. Wu, Q. Xie, M. A. Lysak *et al.*, 2013 Deciphering the diploid ancestral genome of the mesohexaploid *Brassica rapa*. Plant Cell 25: 1541–1554.

Copenhaver, G. P., 2005 A compendium of plant species producing pollen tetrads. J. N. C. Acad. Sci. 121: 17–35.

Copenhaver, G. P., K. Nickel, T. Kuromori, M. I. Benito, S. Kaul *et al.*, 1999 Genetic definition and sequence analysis of *Arabidopsis* centromeres. Science 286: 2468–2474.

Copenhaver, G. P., K. C. Keith, and D. Preuss, 2000 Tetrad analysis in higher plants. A budding technology. Plant Physiol. 124: 7–15.

Cousin, A., and M. Nelson, 2009 Twinned microspore-derived embryos of canola (*Brassica napus* L.) are genetically identical. Plant Cell Rep. 28: 831–835.

Cuenca, J., Y. Froelicher, P. Aleza, J. Juarez, L. Navarro *et al.*, 2011 Multilocus half-tetrad analysis and centromere mapping in citrus: evidence of SDR mechanism for 2n megagametophyte production and partial chiasma interference in mandarin cv 'Fortune'. Heredity 107: 462–470.

De Storme, N., and D. Geelen, 2013 Sexual polyploidization in plants–cytological mechanisms and molecular regulation. New Phytol. 198: 670–684.

De Storme, N., and A. S. Mason, 2014 Plant speciation through chromosome instability and ploidy change: Cellular mechanisms, molecular factors and evolutionary relevance. Current Plant Biology 1: 10–33.

De Storme, N., G. P. Copenhaver, and D. Geelen, 2012 Production of diploid male gametes in *Arabidopsis* by cold-induced destabilization of postmeiotic radial microtubule arrays. Plant Physiol. 160: 1808–1826.

De Storme, N., L. Zamariola, M. Mau, T. F. Sharbel, and D. Geelen, 2013 Volume-based pollen size analysis: an advanced method to assess somatic and gametophytic ploidy in flowering plants. Plant Reprod. 26: 65–81.

Fulton, T. M., J. Chunwongse, and S. D. Tanksley, 1995 Microprep protocol for extraction of DNA from tomato and other herbaceous plants. Plant Mol. Biol. Rep. 13: 207–209.

Han, F. P., J. C. Lamb, and J. A. Birchler, 2006 High frequency of centromere inactivation resulting in stable dicentric chromosomes of maize. Proc. Natl. Acad. Sci. USA 103: 3238–3243.

Hosouchi, T., N. Kumekawa, H. Tsuruoka, and H. Kotani, 2002 Physical map-based sizes of the centromeric regions of *Arabidopsis thaliana* chromosomes 1, 2, and 3. DNA Res. 9: 117–121.

Howell, E. C., G. Barker, G. H. Jones, M. J. Kearsey, G. King *et al.*, 2002 Integration of the cytogenetic and genetic linkage maps of *Brassica oleracea*. Genetics 161: 1225–1234.

Hubert, S., E. Cognard, and D. Hedgecock, 2009 Centromere mapping in triploid families of the Pacific oyster *Crassostrea gigas* (Thunberg). Aquaculture 288: 172–183.

Johnson, S. L., D. Africa, S. Horne, and J. H. Postlethwait, 1995 Half-tetrad analysis in zebrafish: mapping the ros mutation and the centromere of linkage group I. Genetics 139: 1727–1735.

Koo, D. H., P. Plaha, Y. P. Lim, Y. Hur, and J. W. Bang, 2004 A high-resolution karyotype of *Brassica rapa* ssp *pekinensis* revealed by pachytene analysis and multicolor fluorescence in situ hybridization. Theor. Appl. Genet. 109: 1346–1352.

Koo, D. H., C. P. Hong, J. Batley, Y. S. Chung, D. Edwards *et al.*, 2011 Rapid divergence of repetitive DNAs in *Brassica* relatives. Genomics 97: 173–185.

Krzywinski, M., J. Schein, I. Birol, J. Connors, R. Gascoyne *et al.*, 2009 Circos: an information aesthetic for comparative genomics. Genome Res. 19: 1639–1645.

Leflon, M., F. Eber, J. C. Letanneur, L. Chelysheva, O. Coriton *et al.*, 2006 Pairing and recombination at meiosis of *Brassica rapa* (AA) × *Brassica napus* (AACC) hybrids. Theor. Appl. Genet. 113: 1467–1480.

Lim, K.-B., M. S. Ramanna, J. H. de Jong, E. Jacobsen, and J. M. van Tuyl, 2001 Indeterminate meiotic restitution (IMR): a novel type of meiotic nuclear restitution mechanism detected in interspecific lily hybrids by GISH. Theor. Appl. Genet. 103: 219–230.

Lim, K. B., H. de Jong, T. J. Yang, J. Y. Park, S. J. Kwon *et al.*, 2005 Characterization of rDNAs and tandem repeats in the heterochromatin of *Brassica rapa*. Mol. Cells 19: 436–444.

Lim, K. B., T. J. Yang, Y. J. Hwang, J. S. Kim, J. Y. Park *et al.*, 2007 Characterization of the centromere and peri-centromere

retrotransposons in *Brassica rapa* and their distribution in related *Brassica* species. Plant J. 49: 173–183.
Lin, B. Y., S. J. Chang, and H. M. Lin, 2001 RFLP mapping of the centromere of chromosomes 1, 6 and 9 by B-A translocations in maize. Bot. Bull. Acad. Sin. 42: 273–279.
Liu, L. S., J. O. Tong, W. J. Guo, and X. M. Yu, 2013 Microsatellite-centromere mapping in bighead carp (*Aristichthys nobilis*) using gynogenetic diploid families. Aquacult. Res. 44: 1470–1488.
Liu, Y. L., H. D. Su, J. L. Pang, Z. Goo, X. J. Wang *et al.*, 2015 Sequential de novo centromere formation and inactivation on a chromosomal fragment in maize. Proc. Natl. Acad. Sci. USA 112: E1263–E1271.
Ludlow, C. L., A. C. Scott, G. A. Cromie, E. W. Jeffery, A. Sirr *et al.*, 2013 High-throughput tetrad analysis. Nat. Methods 10: 671.
Mallet, J., 2007 Hybrid speciation. Natl. Rev. 446: 279–283.
Martinez, P., M. Hermida, B. G. Pardo, C. Fernandez, J. Castro *et al.*, 2008 Centromere-linkage in the turbot (*Scophthalmus maximus*) through half-tetrad analysis in diploid meiogynogenetics. Aquaculture 280: 81–88.
Mason, A. S., and J. C. Pires, 2015 Unreduced gametes: meiotic mishap or evolutionary mechanism? Trends Genet. 31: 5–10.
Mason, A. S., M. N. Nelson, M.-C. Castello, G. Yan, and W. A. Cowling, 2011a Genotypic effects on the frequency of homoeologous and homologous recombination in *Brassica napus* × *B. carinata* hybrids. Theor. Appl. Genet. 122: 543–553.
Mason, A. S., M. N. Nelson, G. J. Yan, and W. A. Cowling, 2011b Production of viable male unreduced gametes in *Brassica* interspecific hybrids is genotype specific and stimulated by cold temperatures. BMC Plant Biol. 11: 103.
Mason, A. S., G. J. Yan, W. A. Cowling, and M. N. Nelson, 2012 A new method for producing allohexaploid *Brassica* through unreduced gametes. Euphytica 186: 277–287.
Mason, A. S., J. Batley, P. E. Bayer, A. Hayward, W. A. Cowling *et al.*, 2014a High-resolution molecular karyotyping uncovers pairing between ancestrally related *Brassica* chromosomes. New Phytol. 202: 964–974.
Mason, A. S., M. N. Nelson, J. Takahira, W. A. Cowling, G. Moreira Alves *et al.*, 2014b The fate of chromosomes and alleles in an allohexaploid *Brassica* population. Genetics 197: 273–283.
Mason, A. S., J. Takahira, C. Atri, B. Samans, A. Hayward *et al.*, 2015 Microspore culture reveals complex meiotic behaviour in a trigenomic *Brassica* hybrid. BMC Plant Biol. 15: 173.
Mather, K., and G. H. Beale, 1942 The calculation and precision of linkage values from tetrad analysis. J. Genet. 43: 1–30.
Metzker, M. L., 2010 Sequencing technologies: the next generation. Nat. Rev. Genet. 11: 31–46.
Mun, J. H., S. J. Kwon, Y. J. Seol, J. A. Kim, M. Jin *et al.*, 2010 Sequence and structure of *Brassica rapa* chromosome A3. Genome Biol. 11: R94.
Nasuda, S., S. Hudakova, I. Schubert, A. Houben, and T. R. Endo, 2005 Stable barley chromosomes without centromeric repeats. Proc. Natl. Acad. Sci. USA 102: 9842–9847.
Nelson, M. N., A. S. Mason, M. C. Castello, L. Thomson, G. J. Yan *et al.*, 2009 Microspore culture preferentially selects unreduced (2n) gametes from an interspecific hybrid of *Brassica napus* L. x *Brassica carinata* Braun. Theor. Appl. Genet. 119: 497–505.
Nie, H. T., Q. Li, and L. F. Kong, 2011 Microsatellite-centromere mapping in sea cucumber (*Apostichopus japonicus*) using gynogenetic diploid families. Aquaculture 319: 67–71.
Nie, H. T., Q. Li, and L. F. Kong, 2012 Centromere mapping in the Pacific abalone (*Haliotis discus hannai*) through half-tetrad analysis in gynogenetic diploid families. Anim. Genet. 43: 290–297.
Nomura, K., K. Morishima, H. Tanaka, T. Unuma, K. Okuzawa *et al.*, 2006 Microsatellite-centromere mapping in the Japanese eel (*Anguilla japonica*) by half-tetrad analysis using induced triploid families. Aquaculture 257: 53–67.
Olin-Fatih, M., and W. K. Heneen, 1992 C-banded karyotypes of *Brassica campestris*, *Brassica oleracea*, and *Brassica napus*. Genome 35: 583–589.
Osborn, T. C., D. V. Butrulle, A. G. Sharpe, K. J. Pickering, I. A. Parkin *et al.*, 2003 Detection and effects of a homeologous reciprocal transposition in *Brassica napus*. Genetics 165: 1569–1577.
Pan, G., Y. Zhou, L. C. Fowke, and H. Wang, 2004 An efficient method for flow cytometric analysis of pollen and detection of 2n nuclei in *Brassica napus* pollen. Plant Cell Rep. 23: 196–202.
Park, T. H., J. B. Kim, R. C. B. Hutten, H. J. van Eck, E. Jacobsen *et al.*, 2007 Genetic positioning of centromeres using half-tetrad analysis in a 4x-2x cross population of potato. Genetics 176: 85–94.
Parkin, I. A. P., A. G. Sharpe, D. J. Keith, and D. J. Lydiate, 1995 Identification of the A and C genomes of amphidiploid *Brassica napus* (oilseed rape). Genome 38: 1122–1131.
Parkin, I. A., C. Koh, H. Tang, S. J. Robinson, S. Kagale *et al.*, 2014 Transcriptome and methylome profiling reveals relics of genome dominance in the mesopolyploid *Brassica oleracea*. Genome Biol. 15: R77.
Raemakers, C. J. J. M., E. Jacobsen, and R. G. F. Visser, 1995 Secondary somatic embryogenesis and applications in plant breeding. Euphytica 81: 93–107.
Ramanna, M. S., and E. Jacobsen, 2003 Relevance of sexual polyploidization for crop improvement: a review. Euphytica 133: 3–18.
Ramsey, J., and D. W. Schemske, 1998 Pathways, mechanisms, and rates of polyploid formation in flowering plants. Annu. Rev. Ecol. Syst. 29: 467–501.
Rudd, M. K., and H. F. Willard, 2004 Analysis of the centromeric regions of the human genome assembly. Trends Genet. 20: 529–533.
Schneerman, M. C., W. S. Lee, G. Doyle, and D. F. Weber, 1998 RFLP mapping of the centromere of chromosome 4 in maize using isochromosomes for 4S. Theor. Appl. Genet. 96: 361–366.
Takahira, J., A. Cousin, M. N. Nelson, and W. A. Cowling, 2011 Improvement in efficiency of microspore culture to produce doubled haploid canola (*Brassica napus* L.) by flow cytometry. Plant Cell Tissue Organ Cult. 104: 51–59.
Tavoletti, S., E. T. Bingham, B. S. Yandell, F. Veronesi, and T. C. Osborn, 1996 Half tetrad analysis in alfalfa using multiple restriction fragment length polymorphism markers. Proc. Natl. Acad. Sci. USA 93: 10918–10922.
Veilleux, R., 1985 Diploid and polyploid gametes in crop plants: mechanisms of formation and utilization in plant breeding. Plant Breed. Rev. 3: 253–288.
Wang, G. X., Q. Y. He, F. Liu, Z. K. Cheng, P. B. Talbert *et al.*, 2011 Characterization of CENH3 proteins and centromere-associated DNA sequences in diploid and allotetraploid *Brassica* species. Chromosoma 120: 353–365.
Xiong, Z., and J. C. Pires, 2011 Karyotype and identification of all homoeologous chromosomes of allopolyploid *Brassica napus* and its diploid progenitors. Genetics 187: 37–49.
Zhang, W. L., B. Friebe, B. S. Gill, and J. M. Jiang, 2010 Centromere inactivation and epigenetic modifications of a plant chromosome with three functional centromeres. Chromosoma 119: 553–563.
Zhao, H. Y., and T. P. Speed, 1998 Statistical analysis of half-tetrads. Genetics 150: 473–485.

Communicating editor: A. Houben

GENETICS

Supporting Information
www.genetics.org/lookup/suppl/doi:10.1534/genetics.115.183210/-/DC1

Centromere Locations in *Brassica* A and C Genomes Revealed Through Half-Tetrad Analysis

Annaliese S. Mason, Mathieu Rousseau-Gueutin, Jérôme Morice, Philipp E. Bayer, Naghmeh Besharat, Anouska Cousin, Aneeta Pradhan, Isobel A. P. Parkin, Anne-Marie Chèvre, Jacqueline Batley, and Matthew N. Nelson

DOI: 10.1534/genetics.115.183210

Table S1. Genotypes and production methods to obtain first division restitution (FDR) 2n-gamete derived progeny. For a summary of crossability between different genotypes to produce AABC and CCAB hybrids, see Mason et al. (2010). (.xlsx, 15 KB)

Available for download as a .xlsx file at
www.genetics.org/lookup/suppl/doi:10.1534/genetics.115.183210/-/DC1/TableS1.xlsx

Table S2. Centromere-flanking SNP markers, exact sequence locations and putative inversions or rearrangements in the in the B. napus reference (Darmor v4.1) relative to the genotypes used in this study. (.xlsx, 16 KB)

Available for download as a .xlsx file at
www.genetics.org/lookup/suppl/doi:10.1534/genetics.115.183210/-/DC1 /TableS2.xlsx